Environ. Sci. Technol. **2007**, *41,* 3984−3990

Predicted Secondary Organic Aerosol Concentrations from the Oxidation of Isoprene in the Eastern United States

TIMOTHY E. LANE† AND SPYROS N. PANDIS*,†,‡

Department of Chemical Engineering, Carnegie Mellon University, Pittsburgh, Pennsylvania 15213, and Department of Chemical Engineering, University of Patras, Patra, 26500, Greece

Isoprene, the most abundant non-methane hydrocarbon emitted into the troposphere, has generally not been considered a major source of SOA due to the relatively high volatility of its oxidation products. In this study, the SOA formed from the oxidation of isoprene is predicted using a three-dimensional chemical transport model, PMCAMx, across the eastern U.S. for July, October, January, and April 2001−2002. The variability of the measured SOA yields in the available smog chamber studies is captured by combining the base case scenario with upper and lower bound estimates of the measurements. For the base case simulation, the predicted annual average isoprene SOA concentration in the southeast is 0.09 μg m^{-3} (bounds 0.04−0.23 μg m^{-3}). Isoprene is predicted to produce 70% less SOA across the entire domain for spring and fall than during the summer and negligible amounts of SOA during the winter. During the summer, the average concentrations in the northeast are predicted to be 0.11 μg m^{-3} (bounds 0.04−0.31 μg m^{-3}) and in the southeast 0.19 μg m^{-3} (bounds 0.11−0.58 μg m^{-3}). PMCAMx predictions are compared to available measurements of some isoprene SOA components in North Carolina and New York State. These modeling results suggest that on an annual basis isoprene oxidation is a small but non-negligible organic aerosol source in the eastern U.S. Its contribution is relatively more important during the summer and in the southeast U.S.

1. Introduction

Several recent studies have suggested that isoprene may be an important source of SOA (*1*−*3*). Claeys et al. (*1*) measured significant concentrations of tetrols in the Amazon and provided strong evidence that these low vapor pressure compounds were formed during the atmospheric oxidation of isoprene (*2*, *3*). With a global emission rate of 500 Tg yr^{-1}, isoprene may produce appreciable amounts of SOA even with low SOA yields (*4*). Clayes et al. (*1*) estimated an annual SOA global source strength of 2 Tg yr^{-1} from the oxidation of isoprene. Recent studies suggest that isoprene has SOA mass yields ranging between 0 and 5%, depending on the amount of isoprene reacted (*3*, *5*−*10*).

The chamber studies of Pandis et al. (*5*), Edney et al. (*3*), Kroll et al. (*6*), Kroll et al. (*7*), Ng et al. (*8*), Kliendeinst et al. (*9*), and Dommen et al. (*10*) have investigated the SOA formed directly during the photooxidation of isoprene. Due to differing experimental conditions, such as temperature, relative humidity, seed loading, NO_x and SO_2 levels, etc., varying SOA yields were measured for different amounts of isoprene reacted. Edney et al. (*3*) and Kliendeinst et al. (*9*) suggested that the isoprene SOA yields are higher when H_2SO_4 is present in the particulate phase. The SOA mass yields from the oxidation of isoprene increased by a factor of 14, from 0.2% to 2.8%, in the presence of a strong acid (*3*). However, the ambient aerosol in continental areas rarely contains pure H_2SO_4 due to the presence of NH_3 (*11*). Kroll et al. (*6*, *7*) reported that the SOA mass yields from the photooxidation of isoprene range from 0.9 to 5.5% in high NO_x conditions. Under low (no) NO_x conditions, Kroll et al. (*7*) measured SOA mass yields ranging from 0.9 to 3.6%. Ng et al. (*8*) measured the real-time SOA formation during the photooxidation of 500 ppb of isoprene at a VOC/NO_x ratio of 1.8. The final mass yield at the end of the experiment was 2%, assuming a density of 1.25 g cm^{-3}. Dommen et al. (*10*) measured SOA mass yields as high as 5% and observed the formation of oligomers in the aerosol from isoprene/NO_x photooxidation.

Other studies suggest that isoprene can contribute to ambient SOA by heterogeneous reactions under acidic conditions (*12*) or through polymerization of second generation oxidation products (*13*). Through model simulations, Ervens et al. (*14*) and Lim et al. (*15*) suggested that cloud processing of water-soluble isoprene oxidation products may also contribute to the formation of SOA. According to Lim et al. (*15*), isoprene can contribute at least 1.6 Tg yr^{-1} of SOA on a global scale through cloud processing.

Isoprene may form organic aerosol through a number of pathways. In this study, the base case parametrization for the oxidation of isoprene uses the SOA mass yields and saturation concentrations proposed by Pandis et al. (*5*) together with the yield equation developed by Odum et al. (*16*). Temperature dependence is added to the corresponding saturation concentrations to estimate the isoprene SOA concentration. Two simulations are performed using the base case parametrization to predict the isoprene SOA concentrations dependent on whether the primary organic aerosol (POA) is included in the organic solution (*16*−*19*). Given the uncertainty surrounding the processes leading to SOA formation, lower and upper bound parametrizations were used to estimate the range of expected isoprene SOA concentrations. The lower bound parametrization uses the base case parametrization at 30 °C without a temperature dependence and without the POA included in the organic solution, while the upper bound is calculated using a constant 2% SOA mass yield.

For each scenario, a three-dimensional chemical transport model, PMCAMx, is used to predict the isoprene SOA concentrations across the eastern United States for four different simulation periods: July 12−28, 2001; October 1−17, 2001; January 1−17, 2002; and April 1−17, 2002. The predicted base case isoprene SOA concentrations with the POA included in the organic solution are compared to available ambient tetrol concentrations measured in Research Triangle Park, NC (*20*) and Potsdam, NY (*21*). The predicted upper and lower bound isoprene SOA concentrations give an estimate of the range of expected isoprene SOA concentrations across the eastern U.S. for each season. Although there are significant uncertainties associated with the predicted base case isoprene SOA concentrations, the seasonal variations for isoprene SOA across the eastern U.S. are quantified and discussed.

* Corresponding author phone: (412)268-3531; fax: (412)268-7139; e-mail: spyros@andrew.cmu.edu.
† Carnegie Mellon University.
‡ University of Patras.

10.1021/es061312q CCC: $37.00
Published on Web 04/24/2007

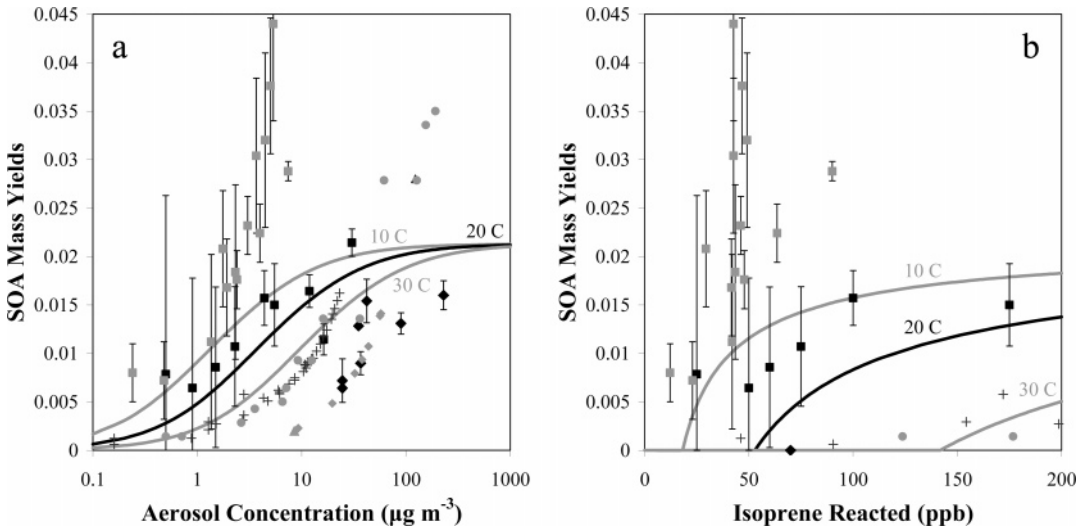

FIGURE 1. Measured and predicted isoprene SOA yields (a) versus total organic aerosol concentration and (b) versus atmospheric concentrations of isoprene reacted. Predicted SOA yields using the base case parametrization at 10 °C, 20 °C, and 30 °C. Measured SOA yields are from (♦) ref *5*, (■) ref *6*, (gray □) ref *7*, (+) ref *8*, (gray ◇) ref *9*, (●) ref *10*, and ref *4* with (▲) and without (gray △) SO_2 assuming a density of 1.0 g cm^{-3}.

2. SOA Modeling

The chemical reaction pathways for atmospheric VOC oxidation are complex, and the resulting oxidation products are both numerous and difficult to measure. Laboratory studies of secondary organic aerosol formation from the oxidation of specific VOCs have mostly measured the total SOA mass yields. The fractional yield (Y) of SOA produced from the oxidation of a VOC is defined as

$$Y = \frac{M_o}{\Delta VOC} \tag{1}$$

where M_o ($\mu g\ m^{-3}$) is the mass concentration of SOA produced from the reaction of ΔVOC ($\mu g\ m^{-3}$) of gaseous VOC.

Experimentally measured Y versus M_o data are fitted with a multiple-product model, using the following equation

$$Y = \sum_i Y_i = \sum_i M_o \left(\frac{\alpha_i}{M_o + c_i^*} \right) \tag{2}$$

where α_i is the mass based stoichiometric coefficient for product i, and c_i^* is the effective saturation concentration in $\mu g\ m^{-3}$ of pure i (*16*). Odum et al. (*16*) showed that SOA yields for an individual VOC measured in a smog chamber agree well with eq 2. This agreement shows that the formation of SOA can be modeled by assuming the formation of a pseudoideal solution by the condensable oxidation products of various VOCs (*16*−*19*). Each condensable product satisfies the mass balance

$$c_{t,i} = c_{g,i} + c_{aer,i} = \frac{\alpha_i MW_i}{MW_{VOC}} \Delta VOC \tag{3}$$

where $c_{t,i}$, $c_{g,i}$, and $c_{aer,i}$ are the total, gas-phase, and aerosol-phase concentration of species i, respectively, and MW_i and MW_{VOC} are the molecular weights of compound i and the VOC. The gas-phase concentrations will satisfy

$$c_{g,i} = \gamma_i x_i c_i^o \quad \text{for } i = 1,...,n \tag{4}$$

where x_i is the mole fraction of compound i in the organic solution, c_i^o is the saturation concentration of pure i, and γ_i is the activity coefficient of the species i. The effective saturation concentration, which is determined from laboratory experiments, is defined as $c_i^* = \gamma_i c_i^o$. In order to solve for the aerosol concentrations of n species, the above equations are combined to yield a system of n equations with n unknowns

$$c_{aer,i} = c_{t,i} - \frac{\dfrac{c_{aer,i}\, c_i^*}{MW_i}}{\displaystyle\sum_{j=1}^{n} \frac{c_{aer,j}}{MW_j} + \frac{c_{POA}}{MW_{POA}}} \quad \text{for } i = 1,\ n \tag{5}$$

where c_{POA} is the concentration of the POA, and MW_{POA} is its average molecular weight. When the POA is not included in the organic solution, the concentration of the POA is set to zero for the aerosol calculations. Within the partitioning model, the Clausius-Clapeyron equation is used for the effective saturation concentration to account for changes in temperature (*22*, *23*).

The base case parametrization uses the Pandis et al. (*5*) mass yields and saturation concentrations in eq 2. The SOA mass yields are 0.0107, 0.0036, and 0.007 with effective saturation concentrations at 298 K of 3.73, 4.04, and 19.28 $\mu g\ m^{-3}$, respectively. The molecular weight and enthalpy of vaporization for all three products were set at 136 g mol^{-1} and 73 kJ mol^{-1} (*22*). With enthalpy of vaporization for SOA species ranging from 42−156 kJ mol^{-1} the selected 73 kJ mol^{-1} is a reasonable choice. Figure 1 compares the predicted SOA yields at different concentrations of total organic aerosol and isoprene reacted to measured SOA yields from refs *5*, *3*, and *6*−*10* assuming a density of 1.0 g cm^{-3}. The SOA yields from refs *5* and *3* were measured at approximately 30 °C, while the SOA yields from refs *6*−*10* were measured at 20 °C. Kliendeinst et al. (*9*) measured the SOA mass yields at 25 °C. While the base case parametrization does not match exactly any of these studies, it is a reasonable representation of their results across the wide range of conditions used. To capture the variability of these results, we rely on upper and lower bound scenarios.

The approximate lower bound was set as the base case parametrization at 30 °C without temperature dependence (Figure 1b). At atmospheric levels of isoprene reacted, the lower bound predicts similar SOA mass yields as the measurements of Dommen et al. (*10*) performed at 20 °C (Figure 1). If less than 140 ppb of isoprene are reacted in the

laboratory, the lower bound expression predicts an SOA mass yield of zero. However, in the atmosphere a fraction of the corresponding semivolatile vapors will dissolve in the existing organic aerosol phase giving nonzero yields at all reacted isoprene levels. For the calculation of the lower bound we assume that the produced SOA will form a solution with the other SOA compounds but not with the primary organic aerosol.

The upper bound, which is set as a constant 2% SOA mass yield, is around the maximum SOA mass yields measured by Kroll et al. (*6*). This is consistent with the maximum SOA mass yield predicted by the base case parametrization at very high values of reacted isoprene or existing organic aerosol. Excluding the SOA yields measured by Kroll et al. (*7*), the maximum SOA yield that has been measured at reacted isoprene levels less than 500 ppb is also approximately 2% (Figure 1). The upper bound will predict higher SOA yields than measured by Kroll et al. (*7*) at low organic aerosol concentrations (less than 2 μg m^{-3}). For this scenario the SOA compounds are assumed to have zero vapor pressure at all temperatures. The results of this upper bound scenario can be easily scaled to different values of the maximum constant yield. For example, if one assumes a constant yield of 4% instead of the 2% used here, the corresponding concentrations can be calculated by multiplying our upper bound results by a factor of 2.

3. PMCAMx

PMCAMx is a three-dimensional chemical transport model which uses the framework of CAMx (*24*) to simulate horizontal and vertical advection, horizontal and vertical dispersion, wet and dry deposition, and gas-phase chemistry. Three aerosol modules have been implemented in PMCAMx to describe inorganic and organic aerosol dynamics and aerosol-cloud interactions using an operator-splitting approach (*25*). PMCAMx tracks 13 different aerosol species: sulfate, nitrate, ammonium, aerosol water content, four secondary organic aerosol species, sodium, chloride, primary organic aerosol, primary elemental carbon, and all primary inert material. The size distribution of each aerosol species has ten size sections, ranging from 40 nm to 40 μm.

For this study, PMCAMx is applied to four 17-day periods in the eastern U.S. starting on July 12, 2001; October 1, 2001; January 1, 2002; and April 1, 2002. The modeling domain covers a 3492 $\times$ 3240 km region in the eastern U.S. with 36 $\times$ 36 km grid resolution with 14 vertical levels up to 6 km (*25*). Inputs to the model include horizontal wind components, temperature, pressure, water vapor, vertical diffusivity, clouds, and rainfall, all created using the meteorological model MM5 (*25*, *26*). The chemistry mechanism used in PMCAMx is the Carbon Bond mechanism version 4 (*24*, *27*). The LADCO BaseE inventory (*24*) is used for the emission inputs for PMCAMx.

According to the emission inventory, the highest average isoprene emission rate is 70 kg km^{-2} day^{-1} during July in southeastern Oklahoma. January has the lowest maximum emission rate, 5 kg km^{-2} day^{-1}. April and October have comparable isoprene emissions, with the maximum emission rate near 20 kg km^{-2} day^{-1}. For all periods, the isoprene emission rates are highest in the southeastern U.S. Isoprene is only emitted during the daytime when sunlight is present.

Lane et al. (*29*), Gaydos et al. (*25*), and Karydis et al. (*30*) have compared the predicted organic carbon concentrations across the eastern U.S. to measured organic carbon concentrations from the EPA Speciation Trends Network (STN) and the Interagency Monitoring of Protected Visual Environments (IMPROVE). During the July simulation period, the predicted organic carbon underpredicts the observed organic aerosol levels with a mean bias of $-0.2\,\mu$g m^{-3} (*30*). According to Karydis et al. (*30*), the mean bias for predicted total organic mass for the months of October, January, and April compared to STN and IMPROVE measurements is 0.17, 0.92, and 0.27 μg m^{-3}. During these periods the model is overpredicting on average the organic aerosol concentrations.

4. Results and Discussion

Across the entire modeling domain, the average primary organic aerosol (POA) concentration at the ground level during the 17-day July 2001 simulation period is 1.1 μg m^{-3} (*29*). The domain average ground-level POA concentrations during the 17-day October, January, and April simulations are higher than for the July simulation at 1.3 μg m^{-3}, 1.6 μg m^{-3}, and 1.5 μg m^{-3}, respectively. With the addition of the POA to the organic solution, more organic aerosol is present to absorb the secondary condensable products.

For July, the predicted domain average total secondary organic aerosol (SOA) concentration at the ground level is 0.7 μg m^{-3} (*29*, *30*). The maximum predicted average total SOA concentration of 2.5 μg m^{-3} occurs above southern Arkansas for the July simulation. In the southeast, the total SOA concentrations are dominated by biogenic SOA, which has a similar spatial distribution to the isoprene SOA. The anthropogenic SOA concentrations are predicted to have high contributions around northern cities. For October, January, and April, the domain average total SOA concentrations are 0.4, 0.2, and 0.4 μg m^{-3} (*30*).

4.1. SOA Produced from Isoprene: Base Case Scenario. The average predicted concentrations of SOA from the oxidation of isoprene using the base case parametrization, with the POA included in the organic solution, for July, October, January, and April, are shown in Figure 2. The monthly and annual average isoprene SOA concentrations in the northeast and southeast are listed in Table 1.

In the southeast, isoprene is predicted to contribute an average of 0.09 μg m^{-3} (bounds 0.04$-$0.23 μg m^{-3}) of SOA annually using the base case. In the northeast, the predicted isoprene SOA concentrations are around 50% less than in the southeast. The annual average predicted isoprene SOA concentration in the northeast for the base case scenario is 0.05 μg m^{-3} (0.01$-$0.11 μg m^{-3}).

The average isoprene SOA concentration is predicted to reach its maximum during the summer. During the July simulation, the predicted average isoprene SOA concentrations are 0.19 μg m^{-3} (0.11$-$0.58 μg m^{-3}) in the southeast and 0.11 μg m^{-3} (0.04$-$0.31 μg m^{-3}) in the northeast using the base case scenario. In January, the average predicted isoprene SOA concentrations in both the northeast and southeast are near zero (0.01 μg m^{-3}). The April and October simulations are predicted to have average isoprene SOA concentrations lower than in July but higher than in January. The average isoprene SOA concentrations for October and April are 0.08 μg m^{-3} (bounds 0.02$-$0.18 μg m^{-3}) and 0.06 μg m^{-3} (0.01$-$0.14 μg m^{-3}) in the southeast and 0.03 μg m^{-3} (0.01$-$0.06 μg m^{-3}) and 0.06 μg m^{-3} (0.01$-$0.09 μg m^{-3}) in the northeast, respectively.

On an annual average basis the concentrations of the isoprene SOA represent a few percent of the total organic aerosol concentration. These concentrations are small but non-negligible. The wintertime values are predicted to be 20 times smaller than those during the summer. Isoprene SOA during the summer in the southeastern U.S. is predicted to contribute 7% of the total organic aerosol. The addition of the isoprene SOA during the summer to the organic aerosol predicted by PMCAMx improves the agreement of the model with the available measurements by correcting the small tendency of the model to underpredict the summertime SOA concentrations. The absolute mean bias between the predicted total organic mass and the IMPROVE and STN measurements was reduced by 0.1 μg m^{-3}.

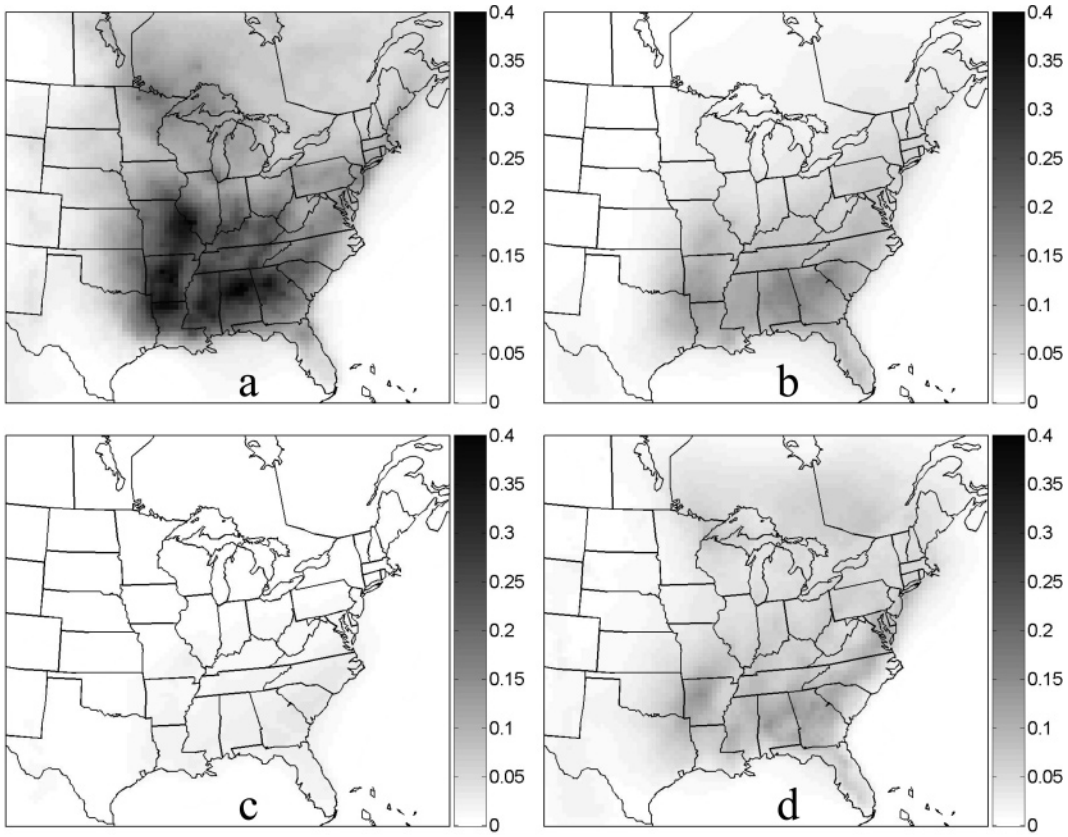

FIGURE 2. Average SOA concentrations from the oxidation of isoprene predicted in the eastern U.S. using the Pandis et al. (*1*) parametrization during (a) July 12−28, 2001, (b) October 1−17, 2001, (c) January 1−17, 2002, and (d) April 1−17, 2002.

TABLE 1. Average Predicted Isoprene SOA Concentrations (μg m^{-3}) in the Southeast and Northeast Subdomains for July 12−28, 2001; October 1−17, 2001; January 1−17, 2002; April 1−17, 2002; and for the Year

scenario	subdomain	July	October	January	April	annual
base case	SE	0.19	0.08	0.01	0.06	0.09
	NE	0.11	0.03	0.00	0.05	0.05
base case w/o POA	SE	0.15	0.05	0.01	0.03	0.06
	NE	0.07	0.02	0.00	0.03	0.03
lower bound	SE	0.11	0.02	0.00	0.01	0.04
	NE	0.04	0.01	0.00	0.01	0.01
upper bound	SE	0.58	0.18	0.02	0.14	0.23
	NE	0.31	0.06	0.01	0.09	0.11

4.2. Upper and Lower Bounds of Isoprene SOA. Figure 3 shows that the predicted isoprene SOA concentrations from the lower and upper bound scenarios have a similar spatial distribution as shown in the base case scenario for all simulation periods. The upper bound scenario, as expected, predicts the highest isoprene SOA concentrations for each simulation period, July being the highest with an average isoprene SOA concentration of 0.58 μg m^{-3} in the southeast. The maximum simulated average concentration in this upper bound scenario during July is 1.1 μg m^{-3} over southern Arkansas (Figure 3). The predicted upper bound isoprene SOA concentrations for April and October are comparable to the base case predictions for July. The maximum average predicted isoprene SOA concentration for the upper bound for October and April are 0.33 μg m^{-3} east of Atlanta, on the Georgia−South Carolina border, and 0.28 μg m^{-3} west of Little Rock, AR, respectively (Figure 3). For January, the maximum average isoprene SOA concentration predicted for the upper bound scenario is only 0.05 μg m^{-3}.

The predicted yearly average isoprene SOA concentrations in the upper bound scenario are 0.11 μg m^{-3} in the northeast and 0.23 μg m^{-3} in the southeast. Henze and Seinfeld (*31*) used a two-product model fit for the low NO_x SOA yields measured by Kroll et al. (*7*) in a global model and predicted the yearly average SOA concentrations. According to Figure 1 from Henze and Seinfeld (*31*), the SOA concentration increased by approximately 0.1 μg m^{-3} in the northeastern U.S. and 0.25 μg m^{-3} in the southeastern U.S. with the addition of isoprene photooxidation, values consistent with our upper bound predictions. This agreement also confirms that our upper bound gives results over this area that are similar with those of the Kroll et al. (*7*) parametrization.

For the lower bound scenario, the maximum average isoprene SOA concentrations for July, October, January, and April are 0.28 μg m^{-3}, 0.05 μg m^{-3}, 0.01 μg m^{-3}, and 0.05 μg m^{-3}, respectively. For July, the lower bound average isoprene SOA concentrations in the northeast and southeast are 0.04 μg m^{-3} and 0.11 μg m^{-3}, respectively. Overall, the lower bound scenario only predicts significant isoprene SOA during July in the southeastern U.S.

4.3. Effect of Primary Organic Aerosol. Using the base case parametrization without the POA included in the organic solution, the maximum average isoprene SOA concentration is 0.31 μg m^{-3} over southern Arkansas during July 12−28, 2001. With the primary organic aerosol added to the organic solution, the predicted isoprene SOA over southern Arkansas increases to 0.36 μg m^{-3}. However, the inclusion of POA in the organic solution provides a maximum average predicted isoprene SOA concentration of 0.44 μg m^{-3} over Birmingham, AL.

The average isoprene SOA concentrations for the base case with and without the POA included in the organic solution are 0.11 and 0.07 in the northeast and 0.19 and 0.15 in the southeast, respectively (Table 1). For October and April, the differences between the maximum average predicted SOA concentration from the base case scenario and the base case

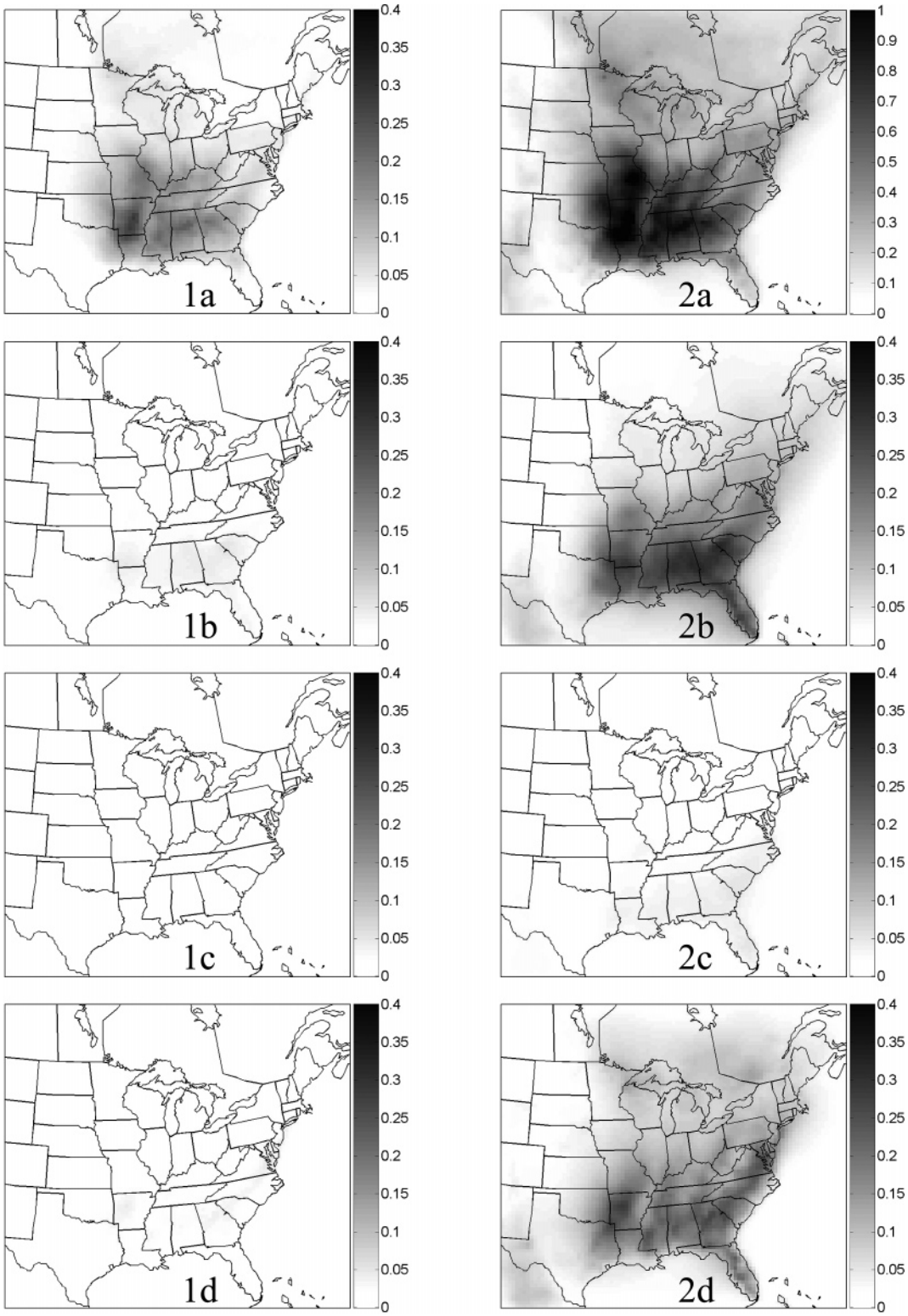

FIGURE 3. The (1) lower and (2) upper bound average SOA concentrations from the oxidation of isoprene predicted in the eastern U.S. during (a) July 12−28, 2001, (b) October 1−17, 2001, (c) January 1−17, 2002, and (d) April 1−17, 2002 (please note the different scale used for the July upper bound).

without the POA included in the organic solution are 0.05 μg m^{-3} and 0.06 μg m^{-3}, respectively. With the addition of the POA to the organic solution, the domain average isoprene SOA concentrations for all four simulation periods increase by 0.02 μg m^{-3}, with the largest effects in the urban areas with high POA concentrations.

4.4. Diurnal Variation. Figure 4a shows the base case average daily isoprene SOA concentrations averaged over each simulation period for Research Triangle Park, NC. The average hourly isoprene SOA concentrations between the four cases for the July simulation for the same area are shown in Figure 4b. In general, the ground level isoprene SOA concentration is predicted to decrease from midnight until sunrise. The isoprene SOA concentrations start increasing at some point after sunrise: January − 11 a.m., April − 6 a.m., October − 8 p.m., and July − 7 a.m. During April, July, and

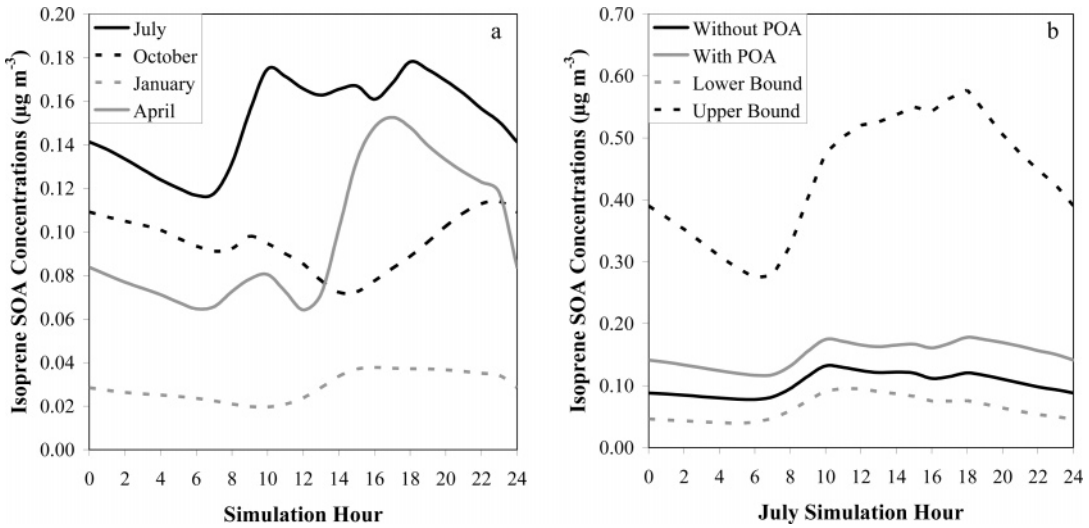

FIGURE 4. Average hourly isoprene SOA concentrations predicted (a) for each scenario during July 2001 and (b) for the base case during each season over Research Triangle Park, NC.

October, the isoprene SOA concentration decreases around 10 a.m. before increasing again in the afternoon. These changes are due to the combined effects of photochemical production during the day, changes in partitioning due to temperature changes, dilution effects, and removal processes. The maximum isoprene SOA concentrations are predicted to occur in the late afternoon and early evening. The different scenarios all predicted similar trends throughout the day for each location.

4.5. Comparison with Observations. Figure 5 compares the minimum, 25th percentile, mean, 75th percentile, and maximum daily average isoprene SOA concentrations predicted using the base case scenario to the daily average tetrol concentrations measured in Research Triangle Park, NC during 2003 (*20*) and in Potsdam, NY during 2005 (*21*). Tetrols represent only a fraction of the isoprene SOA concentration, so these comparisons are relative. The average predicted SOA concentrations show similar trends when compared to the observed tetrol concentrations. The summer months have the highest predicted SOA and measured tetrol concentrations, while the lowest concentrations are during the winter.

Direct comparisons between observed tetrol concentrations and predicted isoprene SOA are difficult because tetrols represent a yet unknown fraction of the isoprene SOA at atmospheric isoprene concentration levels. Kourtchev et al. (*32*) found that tetrols represented approximately 50% of the measured isoprene products during the summer in a boreal forest (Hyytiälä, Finland). However, this factor of 2 could be a low estimate of the isoprene SOA because there could be other major isoprene SOA products not identified in the field. During the fall, Kourtchev et al. (*32*) found that the concentrations of the other isoprene SOA products were below detection levels (practically zero). If the tetrols represent practically all of the isoprene SOA in July, then the predictions of the base case model are consistent with the observations. If the tetrol contribution to the ambient isoprene SOA is much less than 30%, then the upper bound scenario is underpredicting the isoprene SOA during the summer. If this is the case, then either our parametrization in underestimating the isoprene SOA formation under ambient conditions or additional chemical production pathways (e.g., aqueous-phase production) need to be taken into account.

In Potsdam, NY, the observed average fall tetrol concentration was 60% lower than the observed average summer concentration (*21*). The average predicted base case isoprene SOA concentration by PMCAMx in this area in the fall was

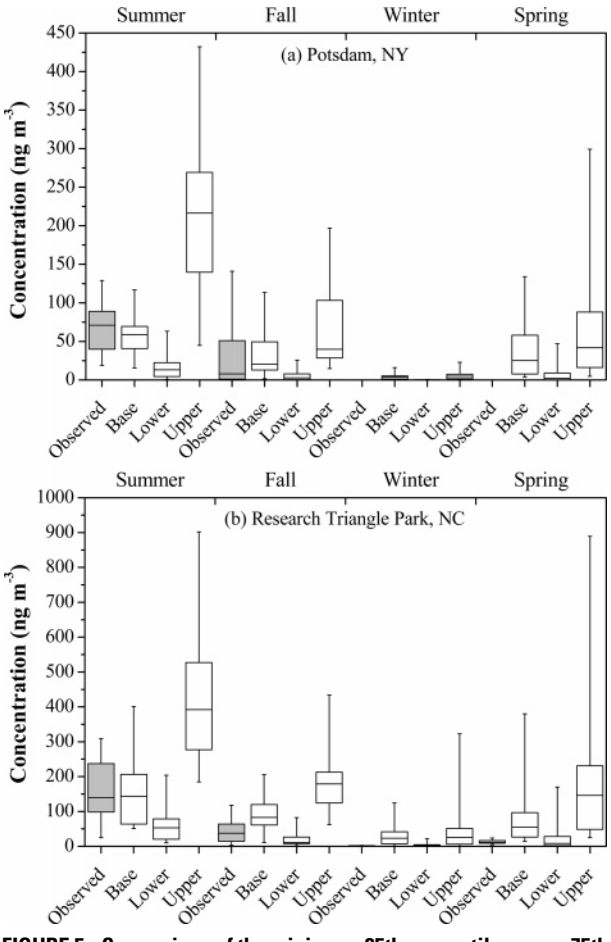

FIGURE 5. Comparison of the minimum, 25th percentile, mean, 75th percentile, and maximum predicted daily average isoprene SOA concentrations from the base case scenario with the tetrol measurements from (a) ref *21* over Potsdam, NY and (b) ref *20* over Research Triangle Park, NC.

40% less than the average summer concentration. In North Carolina the ratio of the average observed fall and spring tetrol concentrations to the summer concentration are 0.3 and 0.1, respectively (*20*). According to the base case scenario, the corresponding PMCAMx ratios in that area are around 0.6 for these seasons. This indicates that the summer concentrations may be underpredicted in that area or the

fall and spring may be overpredicted. Another potential explanation is that the ratio of the tetrols to the total isoprene SOA is not constant during the year. These comparisons should be viewed as preliminary because they do not even refer to the same year. Therefore year-to-year differences can also explain some of these discrepancies. Additional tetrol concentration measurements are necessary together with a better understanding of their contribution to the total isoprene SOA mass concentration.

Acknowledgments

The authors would like to thank the Lake Michigan Air Directors Consortium for providing the meteorological files, the area and point emission files, and the initial and boundary condition files for PMCAMx and P. Hopke and U. Baltensperger for providing the data discussed in refs *10* and *21* before the publication of the papers. This research was supported by the EPA STAR program through the National Center for Environmental Research (NCER) under grant R832162. This paper has not been subject to EPA's required peer and policy review and therefore does not necessarily reflect the views of the Agency. No official endorsement should be inferred.

Literature Cited

(1) Claeys, M.; Graham, B.; Vas, G.; Wang, W.; Vermeylen, R.; Pashynska, V.; Cafmeyer, J.; Guyon, P.; Andreae, M. O.; Artaxo, P.; Maenhaut, W. Formation of secondary organic aerosols through photooxidation of isoprene. *Science* **2004**, *303*, 1173−1176.

(2) Claeys, M.; Wang, W.; Ion, A. C.; Kourchew, I.; Gelencser, A.; Maenhaut, W. Formation of secondary organic aerosols from isoprene and its gas-phase oxidation products through reaction with hydrogen peroxide. *Atmos. Environ.* **2004**, *38*, 4093−4098.

(3) Edney, E. O.; Kleindienst, T. E.; Jaoui, M.; Lewandowski, M.; Offenberg, J. H.; Wang, W.; Claeys, M. Formation of 2-methyl tetrols and 2-methylglyceric acid in secondary organic aerosol from laboratory irradiated isoprene/NO_x/SO_2/air mixtures and their detection in ambient $PM_{2.5}$ samples collected in the eastern United States. *Atmos. Environ.* **2005**, *39*, 5281−5289.

(4) Guenther, A.; Hewitt, C.; Erickson, D.; Fall, R.; Geron, C.; Graedel, T.; Harley, P.; Klinger, L.; Lerdau, M.; McKay, W.; Piersce, T.; Scholes, B.; Steinbrecher, R.; Tallamraju, R.; Taylor, J.; Zimmerman, P. A global model of natural volatile organic compound emissions. *J. Geophys. Res.* **1995**, *100*, 8873−8892.

(5) Pandis, S. N.; Paulson, S. E.; Seinfeld, J. H.; Flagan, R. C. Aerosol formation in the photooxidation of isoprene and β-pinene. *Atmos. Environ.* **1991**, *25A*, 997−1008.

(6) Kroll, J. H.; Ng, N. L.; Murphy, S. M.; Flagan, R. C.; Seinfeld, J. H. Secondary organic aerosol formation from isoprene photooxidation under high-NO_x conditions. *Geophys. Res. Lett.* **2005**, *32*, L18808.

(7) Kroll, J. H.; Ng, N. L.; Murphy, S. M.; Flagan, R. C.; Seinfeld, J. H. Secondary organic aerosol formation from isoprene photooxidation. *Environ. Sci. Technol.* **2006**, *40*, 1869−1877.

(8) Ng, N. L.; Kroll, J. H.; Keywood, M. D.; Bahreini, R.; Varutbangkul, V.; Flagan, R. C.; Seinfeld, J. H.; Lee, A.; Goldstein, A. H. Contribution of first- versus second-generation products to secondary organic aerosols formed in the oxidation of biogenic hydrocarbons. *Environ. Sci. Technol.* **2006**, *40*, 2283−2297.

(9) Kleindienst, T. E.; Edney, E. O.; Lewandowski, M.; Offenberg, J. H.; Jaoui, M. Secondary organic carbon and aerosol yields from the irradiations of isoprene and α-pinene in the presence of NO_x and SO_2. *Environ. Sci. Technol.* **2006**, *40*, 3807−3812.

(10) Dommen, J.; Metzger, A.; Duplissy, J.; Kalberer, M.; Alfarra, M. R.; Gascho, A.; Weingartner, E.; Prevot, A. S. H.; Verheggen, B.; Baltensperger, U. Laboratory observation of oligomers in the aerosol from isoprene/NO_x photooxidation. *Geophys. Res. Lett.* **2006**, *33*, doi: 10.1029/2006GL026523.

(11) Takahama, S.i; Wittig, A. E.; Vayenas, D. V.; Davidson, C. I.; Pandis, S. N. Modeling the diurnal variation of nitrate during the Pittsburgh Air Quality Study. *J. Geophys. Res.* **2004**, *109*, D16S06/1-D16S06/10.

(12) Limbeck, A.; Kulmala, M.; Puxbaum H. Secondary organic aerosol formation in the atmosphere via heterogeneous reaction of gaseous isoprene on acidic particles. *Geophys. Res. Lett.* **2003**, *30*, 1996, doi:10.1029/2003GL017738.

(13) Kalberer, M.; Paulsen, D.; Sax, M.; Steinbacher, M.; Dommen, J.; Prevot, A. S. H.; Fisseha, R.; Weingartner, E.; Frankevich, V.; Zenobi, R.; Baltensperger, U. Identification of polymers as major components of atmospheric organic aerosols. *Science* **2004**, *303*, 1659−1662.

(14) Ervens, B.; Feingold, G.; Frost, G. J.; Kreidenweis, S. M. A modeling study of aqueous production of dicarboxylic acids: 1. Chemical pathways and speciated organic mass production. *J. Geophys. Res.* **2004**, *109*, D15205, doi:10.1029/2003JD004387.

(15) Lim, H.-J.; Carlton, A. G.; Turpin, B. J. Isoprene forms secondary organic aerosol through cloud processing: Model simulations. *Environ. Sci. Technol.* **2005**, *39*, 4441−4446.

(16) Odum, J. R.; Hoffmann, T.; Bowman, F.; Collins, D.; Flagan, R. C.; Seinfeld, J. H. Gas/Particle partitioning and secondary organic aerosol yields. *Environ. Sci. Technol.* **1996**, *30*, 2580−2585.

(17) Odum, J. R.; Jungkamp, T.; Griffin, R. J.; Forstner, H.; Flagan, R. C.; Seinfeld, J. H. Aromatics, reformulated gasoline, and atmospheric organic aerosol formation. *Environ. Sci. Technol.* **1997**, *31*, 1890−1897.

(18) Bowman, F.; Odum, J.; Pandis, S. N.; Seinfeld, J. H. Mathematical model for gas-particle partitioning of secondary organic aerosol. *Atmos. Environ.* **1997**, *31*, 3921−3931.

(19) Strader, R.; Lurmann, F.; Pandis, S. N. Evaluation of secondary organic aerosol formation in winter. *Atmos. Environ.* **1999**, *33*, 4849−4863.

(20) Kleindienst, T.; Edney, E.; Lewandowski, M.; Offenberg, J.; Jaoui, M.; Seinfeld, J. *Formation mechanisms for secondary organic aerosol in ambient air*, European Aerosol Conference, Ghent, Belgium, 2005.

(21) Xia, X.; Hopke, P. K. Seasonal variation of 2-methyltetrols in ambient air samples. *Environ. Sci. Technol.* **2006**, *40*, 6934−6937.

(22) Sheehan, P. E.; Bowman, F. M. Estimated effects of temperature on secondary organic aerosol concentrations. *Environ. Sci. Technol.* **2001**, *35*, 2129−2135.

(23) Takekawa, H.; Minoura, H.; Yamazaki, S. Temperature dependence of secondary organic aerosol formation by photooxidation of hydrocarbons. *Atmos. Environ.* **2003**, *37*, 3413−3424.

(24) Environ. *User's guide to the comprehensive air quality model with extensions (CAMx). Version 4.10*; Report prepared by ENVIRON International Corporation; Novato, CA, 2003.

(25) Gaydos, T. M.; Pinder, R. W.; Koo, B.; Fahey, K. M.; Pandis, S. N. Development and application of a three-dimensional aerosol chemical transport model, PMCAMx. *Atmos. Environ.* **2007**, *41*, 2594−2611.

(26) Grell, G. A., Dudhia, J.; Stauffer, D. R. *A Description of the fifth-generation Penn State/NCAR Mesoscale Model (MM5)*; 1995; NCAR/TN-398+STR. http://www.mmm.ucar.edu/mm5/documents/mm5-desc-doc.html (accessed March 2007).

(27) Gery, M. W.; Whitten, G. Z.; Killus, J. P.; Dodge, M. C. A photochemical kinetics mechanism for urban and regional scale computer modeling. *J. Geophys. Res.* **1989**, *94*, 925−956.

(28) LADCO. *Base E Modeling Inventory*; Midwest Regional Planning Organization: Des Plaines, IL, September 16, 2003. http://www.ladco.org/tech/emis/BaseE/baseEreport.pdf (accessed March 2007).

(29) Lane, T. E.; Pinder, R. W.; Shrivastava, M.; Robinson, A. L.; Pandis, S. N. Source contributions to primary organic aerosol; Comparison of the results of a source-resolved model and the chemical mass balance approach. *Atmos. Environ.*, in press.

(30) Karydis, V. A.; Tsimpidi, A. P.; Pandis, S. N. Evaluation of a three-dimensional Chemical Transport Model (PMCAMx) in the Eastern United States for all four seasons. *J. Geophys. Res.*, in press.

(31) Henze, D. K.; Seinfeld, J. H. Global secondary organic aerosol from isoprene oxidation. *Geophys. Res. Lett.* **2006**, *33*, L09812, doi:10.1029/2006GL025976.

(32) Kourtchev, I.; Ruuskanen, T.; Maenhaut, W.; Kulmala, M.; Claeys, M. Observation of 2-methyltetrols and related photo-oxidation products of isoprene in boreal forest aerosols from Hyytiälä, Finland. *Atmos. Chem. Phys.* **2005**, *5*, 2761−2770.

Received for review June 1, 2006. Revised manuscript received October 16, 2006. Accepted February 27, 2007.

ES061312Q